Vacuum 86 (2012) 623–626

Contents lists available at SciVerse ScienceDirect

Vacuum

journal homepage: www.elsevier.com/locate/vacuum

Tunneling induced decomposition of $Mo(CO)_6$ onto $TiO_2(110)$ surface

Z. Majzik[a,b], N. Balázs[c], L. Robin[d], M. Petukhov[d], B. Domenichini[d], S. Bourgeois[d], A. Berkó[a,c,*]

[a] Department of Physical Chemistry and Material Science, University of Szeged, Dóm tér 7, H-6720 Szeged, Hungary
[b] Department of Thin Films, Institute of Physics of the Academy of Sciences of Czech Republic, Cukrovarnicka 10, Prague 6, 162 53 Czech Republic
[c] Reaction Kinetics Research Laboratory, Institute of Nanochemistry and Catalysis, Chemical Research Center of the Hungarian Academy of Sciences, Pusztaszeri út 59-67, 1525 Budapest, Hungary
[d] Laboratoire Interdisciplinaire Carnot de Bourgogne (ICB) UMR 5209 CNRS, Université de Bourgogne, 9 avenue Alain Savary, Boîte Postale 47870, 21078 Dijon Cedex, France

Keywords:
Scanning tunneling microscopy and spectroscopy
Tunneling current induced local decomposition of $Mo(CO)_6$
Nanoscale lithography

A B S T R A C T

Tunneling induced decomposition of $Mo(CO)_6$ from the gas phase was studied on $TiO_2(110)$ surface by scanning tunneling microscopy (STM) and spectroscopy (STS). The efficiency of the procedure was followed by measuring the dot volume as a proportional indicator of the amount of the decomposed precursor. It was found that below 1×10^{-5} Pa background pressure of $Mo(CO)_6$, there is no measurable effect and above 1×10^{-4} Pa, the nanodot size is too large compared to the curvature of the tip (20–40 nm). A threshold bias of +3.1(±0.1) V on the sample was measured for the decomposition of $Mo(CO)_6$ in gas ambient. In the absence of the precursor, dot formation was observed only above +3.7(±0.2) V, in good agreement with the results reported in our earlier work about nanolithography on clean $TiO_2(110)$ substrate (*E. Kriván, A. Berkó: J. Vac. Sci. & Tech. B* 15(1) (1997)25). By applying voltages in the range of 3.1–3.5 V, a systematic enlargement of the created nanodots was found in the range of 2–20 s of duration and 0.01–1.0 nA of tunneling current. The I–V curves detected on the top of the nanodots have shown that the created features are of insulator character. This observation indicates that the decomposition of $Mo(CO)_6$ is also accompanied by oxidation of the deposited Mo species.

1. Introduction

Electron induced local deposition of metal containing precursors for patterning of oxide or metal surfaces opens the door to the nanoelectronics related application fields, like production of integrated gas sensors [1–3]. Especially, the utilization of the tunneling region of a scanning probe confined to extremely small lateral size (~1 nm^2) is a very promising method for the production of nanodevices [4–7]. In spite of the obvious disadvantage in production speed of this procedure, the lateral resolution can be so high that for certain applications, this method will certainly be the only nanofabrication technique. Recent studies on the adsorption and decomposition of metal carbonyls refer several distinct advantages of their application in the nanolithography: (1) the strict number of the metal atoms contained in this type of molecules and the variability of their composition; (2) the weak bonding of these molecules to the substrates and transformability by electron radiation of low energy into much stronger bonded species (partial decomposition); (3) large cross section for the electron induced decomposition. Accordingly, these properties make metal carbonyls to be excellent precursor also for nanopatterning performed by scanning atom probe techniques (such as STM) [2,6,7]. As concerns $Mo(CO)_6$ chemisorption on $TiO_2(110)$ surface, in a recent work we have shown that this compound adsorbs at 140 K and desorbs below 180 K almost exclusively in molecular form, however, photon irradiation initiates the decomposition of the adsorbed precursor molecules [8]. In order to activate the thermal decomposition of $Mo(CO)_6$, Rizzi et al. used rather drastic conditions: highly defective TiO_2 substrate at high temperature (400–450 °C), reactive oxygen ambient of ~10^{-3} Pa and precursor pressure of ~ 5×10^{-4} Pa [9]. Detailed studies of electron and photon beam induced decomposition of this material on metal and oxide surfaces are in progress in our laboratories.

In this work we present the first results obtained on the tunneling electron induced decomposition of gas phase $Mo(CO)_6$ on a $TiO_2(110)$ surface at room temperature. The efficiency of Mo deposition was followed by the detection of nanodots formed on the substrate.

2. Experimental

The measurements were carried out in a commercial UHV chamber equipped by a room temperature STM head, an electron

* Corresponding author. Department of Physical Chemistry and Material Science, University of Szeged, Dóm tér 7, H-6720 Szeged, Hungary.
E-mail address: aberko@chem.u-szeged.hu (A. Berkó).

0042-207X/$ – see front matter © 2011 Elsevier Ltd. All rights reserved.
doi:10.1016/j.vacuum.2011.08.009

energy analyzer (CMA) and a quadrupole mass spectrometer. Chemically etched tungsten STM tips were applied in this work, although, some comparative experiments were also performed by Pt–Ir tips. The cleanliness of the TiO_2(110) surface was characterized by STM and Auger-electron spectroscopy (AES). The STM measurements were performed in constant current mode with a typical bias/current of $U_b = +1.5$ V (on the sample) and $I_t = 0.2$ nA. The volume of the nanodots deposited onto the oxide probe in $Mo(CO)_6$ ambient ($10^{-5} - 10^{-4}$ Pa) was determined by evaluation of STM images recorded before and after the treatment. The powder-like $Mo(CO)_6$ purchased from Aldrich (purity of 98%) was filled into a glass tube mounted on a fine leak valve and was pumped at room temperature by a turbomolecular pump for 2 h. Before the inlet of the precursor into the STM chamber, a few minutes evacuation cycle was always performed in order to remove CO accumulated in the container tube at room temperature. No extra annealing of the precursor was applied.

The procedure to create an individual nanodot consisted of three steps: (1) finding and imaging of a clean surface region of 20×20 nm^2 containing no extra features; (2) after moving the STM tip to the centre of the region, the tunneling current and bias voltage were stepwise set to the dot-generation values for several second (duration); (3) using the imaging parameters (see above), the region was imaged once again. The new feature detected in the center of the image was identified as the created nanodot. It should be remarked that the appropriate background pressure of the precursor was set to be constant during several cycles of the three-step procedure. Our preliminary experiments have shown that below 10^{-5} Pa background pressure of the precursor, there is no detectable dot formation which could be assigned to tip induced deposition process. It should be remarked that the lateral drift of the tip cannot automatically be compensated in our STM equipment, however, on the basis of our estimation, this effect was not larger than 5–10% of the diameter of the created nanodots through the longest duration applied.

3. Results and discussion

In this work, we present the experimental results of a systematic study on the effect of different fabrication parameters, like background pressure of the precursor, sample-tip bias, tunneling current and treatment duration.

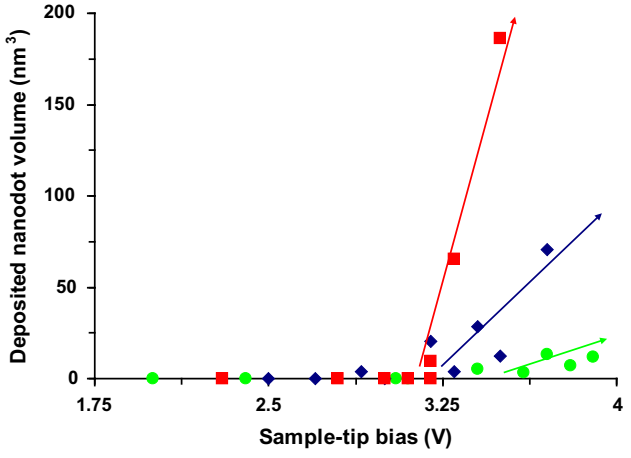

Fig. 1. Change of the nanodot volume created by the decomposition of $Mo(CO)_6$ for three different ambient pressures (●) UHV background ($<1 \times 10^{-7}$ Pa), (◆) 3×10^{-5} Pa and(■) 1×10^{-4} Pa inlet of the precursor. The tunneling current (0.2 nA) and the duration (10 s) were kept constant, the sample-tip bias was varied in the range of 2.0–3.8 V.

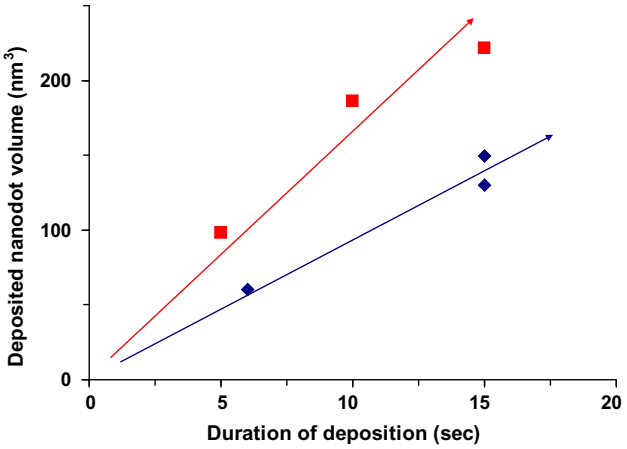

Fig. 2. Change of the nanodot volume created by the decomposition of $Mo(CO)_6$ for two different ambient pressures (◆) 3×10^{-5} Pa and (■) 1×10^{-4} Pa inlet of the precursor. The sample-tip bias (+3.5 V) and the tunneling current (0.2 nA) were kept constant, the duration of the dot creation was varied between 0 and 15 s.

Fig. 1 shows the volume of the created nanodots as a function of the sample-tip bias in the range of 2–4 V for three different cases: for background pressure of $\sim 1 \times 10^{-7}$ Pa and flowing inlet of 3×10^{-5} Pa or 1×10^{-4} Pa $Mo(CO)_6$ accompanied by continuous ion getter pumping. The generation and the detection of the nanodots were performed in the way described above. The treatment duration of 10 s was fixed for each case. It can be seen that in the absence of the precursor, the dot formation is very limited and smaller nanodots (with a volume of 5–10 nm^3) appear only above $+3.7(\pm 0.1)$ V. In the case of introducing 3×10^{-5} Pa $Mo(CO)_6$, dots appear even at $+3.2$ (± 0.1) V and for $+3.7$ V, they are significantly larger than without precursor background. For the inlet of 1×10^{-4} Pa, the dot volume increases very intensively from the threshold bias of $+3.1$ (± 0.1) V (Fig. 1). Assuming that the tip-sample distance is approximately equal to the diameter of a single $Mo(CO)_6$ molecule and the tunneling region is ca. 1 nm^2, roughly 2×10^3 $Mo(CO)_6$ molecules appear in the tunneling region at a pressure of 10^{-4} Pa within 10 s. The volume generated at $+3.4$ V (Fig. 1) is approximately 180 nm^3 which is only a few times more than the aggregate volume of the molecules appearing in the tunneling region (as calculated above). This rough estimation indicates that almost all the molecules appearing in the tunneling

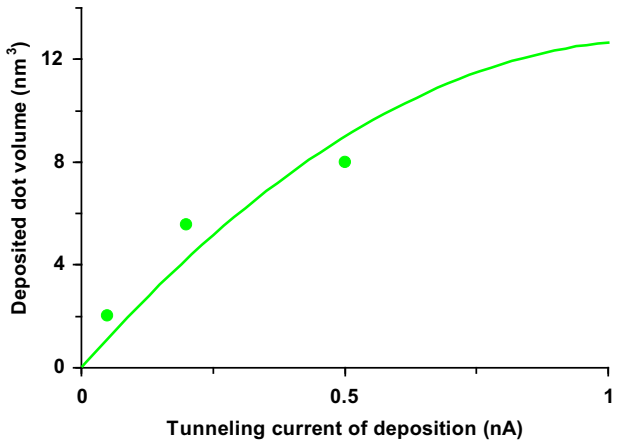

Fig. 3. Change of the nanodot volume created by the decomposition of $Mo(CO)_6$ for 1×10^{-5} Pa inlet of the precursor. The sample-tip bias (+3.2 V) and the duration (10 s) were kept constant, the tunneling current was varied in the range of 0.05–1.0 nA.

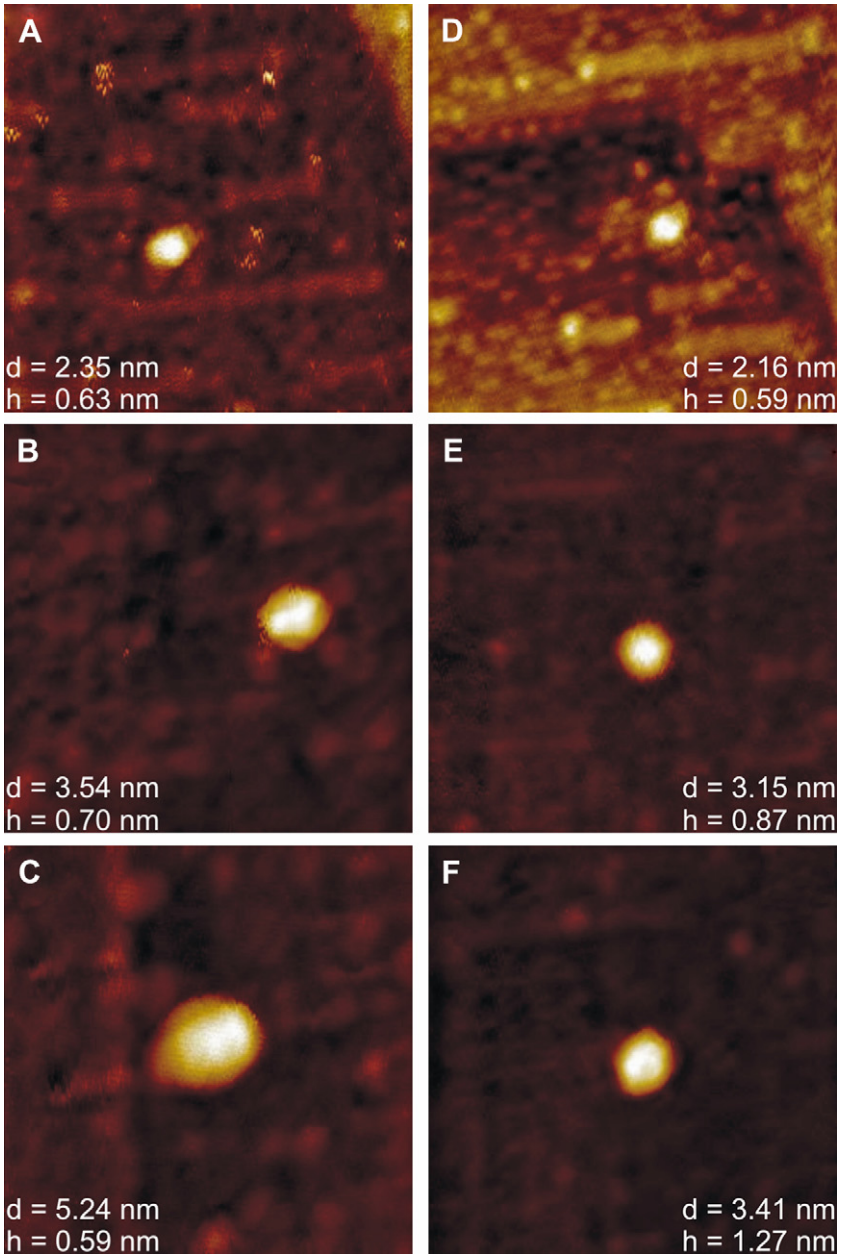

Fig. 4. STM images (20×20 nm^2) of the nanodots created by the decomposition of $Mo(CO)_6$ with different parameters. The effect of the tunneling current (A) 0.02 nA, (B) 0.15 nA, (C) 1.0 nA, while the sample-tip bias (+3.2 V), the duration of the dot creation (10 s) and the inlet pressure of the precursor (10^{-5} Pa) were kept constant. The effect of the treatment duration (D) 5 s, (E) 10 s, (F) 15 s, while the sample-tip bias (+3.2 V), the tunneling current (0.2 nA) and the precursor pressure (10^{-5} Pa) were kept constant.

region will be decomposed. Moreover, the excess of the decomposed amount can be explained by the adsorption-diffusion-decomposition of the molecules on a more extended part of the tip. Taking into account the current flow through the tip-sample gap (10 s, 0.2 nA), the number of electrons participating in the dot generation process is approximately 10^9, which yields a decomposition cross section magnitude of 10^{-5}. This fact suggests that the further increase of the pressure would result in an enhanced decomposition, or in other words, the duration could be significantly decreased at higher pressures for achieving the same effect. The threshold bias of +3.1 V fits well to the lowest ligand–field electron transition in the carbonyl molecule [10]. It can be assumed that the adsorbed molecules decompose more easily than those present in the gas phase. It should be remarked that our similar experiments performed on Au(111) and Cu(110) surfaces (not presented here), indicate nearly the same threshold bias and deposition rate. This observation suggests a substrate independent process. Furthermore, the experiments performed by a Pt–Ir tip indicated that this tip is not so effective as a W tip. The origin of this difference can be rather complex: (i) the adsorption of the precursor on the tip itself may be of decisive importance; (ii) the process can be influenced by the curvature of the tip end; (iii) the electronic effect arising from the different work functions of the two materials may also be crucial. Nevertheless, to distinguish among these effects, a further detailed investigation is needed.

In the subsequent experiments, we have tested the effect of the tunneling current and the treatment duration on dot generation. Fig. 2 shows the change of the dot volume as a function of the duration in the range of 0–15 s for two different inlet pressures of the precursor. As constant parameters, a tunneling current of 0.2 nA

and a bias of +3.5 V were applied in this case. Note, that although longer treatment durations were not checked systematically, deviation from the linear trend was clearly detected. It can be seen that the increase of the precursor pressure leads to an enlargement of the deposited dot volume. This behavior suggests that in order to accelerate the process down to the range of milliseconds (duration), two-three times higher pressure is needed. Nevertheless, the mechanism of the tunneling current induced decomposition of the $Mo(CO)_6$ can be systematically disclosed with the parameters presented here. The variation of the tunneling current in the range of 0.02–1 nA can be seen in Fig. 3, while keeping the bias (+3.2 V), the duration (10 s) and the background $Mo(CO)_6$ pressure (10^{-5} Pa) constant. For these parameters, the volume of the dots is rather small, accordingly, we can get an insight into the very early stage of the deposition process (see also Fig. 4). It can be seen that the dot volume increases intensively with the tunneling current (Fig. 3). The decline of the slope at the higher current values indicates a saturation effect. This feature is in good harmony with the expectation that the limited number of the precursor molecules for a given pressure cannot be compensated by the increase of the tunneling current.

Although the volume of the nanodots is a clear indicator of the deposition activity, the shape of the created nanodot provides also important information about the mechanism of the process. In Fig. 4, three characteristic dots are presented for the change of the tunneling current (A, B, C) and that of the treatment duration (D, E, F). The average diameter (d) and the height (h) of the dots are also indicated in the figure. The increase of the current causes a clear enlargement of the dot diameter, nevertheless, the height of them changes only slightly. Contrary to this, in the case of the duration dependence, both the diameter and the height increase with this parameter. This difference suggests that the increase of the tunneling current substantially accelerates the diffusion of the deposited material resulting in spreading out of the dot. In order to increase the height/diameter aspect ratio of the dots, the application of less current and longer duration can be proposed.

Regarding the composition of the dots generated in Mo-carbonyl background, it is obvious that they are extra deposited structures (no hole formation was observed during our experiments) and probably contain some carbonyl fragments, as well. This assumption is supported by the fact that an extended (repeated) imaging of the dots usually results in a gradual decrease of their volume. Furthermore, the I/V curves recorded on the top of the nanodots indicate an insulator character (not shown here). This means that the oxidation of the deposited Mo species is highly preferred under these circumstances. As a source of oxygen, the TiO_2 substrate may also be determining, however an activated dissociation of CO ligands can not be excluded.

4. Conclusions

In the presence of gas phase $Mo(CO)_6$, Mo-MoO_x nanodots can be reproducibly deposited under a tunneling W-tip on a $TiO_2(110)$ surface. Above a threshold bias of +3.1(±0.1) V (on the sample), the deposited nanodot volume increases systematically with three parameters: the pressure of the precursor in the range of 10^{-5}–10^{-4} Pa, the tunneling current between 0.01 and 1 nA and the duration of 1–15 s. The volume of the nanodots produced with these parameters varies in the range of 10^1–10^3 nm^3.

Acknowledgements

This work was supported by the French-Hungarian Intergovernmental S&T Program (FR-18/2008 TÉT) and by the National Science and Research Fund of Hungary in the frame the grants of K69200 and K81660.

References

[1] Matsui S, Ichihashi T. Appl Phys Lett 1988;53:842.
[2] Henderson MA, Ramsier RD, Yates Jr JT. Surf Sci 1991;259:173.
[3] So SK, Ho W. J Chem Phys 1991;95(1):656.
[4] Marchi F, Tonneau D, Dallaporta H, Safarov V, Bouchiat V, Doppelt P, et al. J Vac Sci Technol B 2000;18(3):1171.
[5] Brückl H, Kretz J, Koops HW, Reiss G. J Vac Sci Technol B 1999;17(4):1350.
[6] Asenjo A, Gómez-Rodrígez JM, Baró AM. Ultramicroscopy 1992;42-44:933.
[7] Femoni C, Iapalucci MC, Kaswalder F, Longoni G, Zacchini S. Coordination Chem Rev 2006;250:1580.
[8] Prunier J, Domenichini B, Li Z, Møller PJ, Bourgeois S. Surf Sci 2007;601:1144.
[9] Rizzi GA, Reeder AE, Agnoli S, Granozzi G. Surf Sci 2006;600:3345.
[10] Chakarov DV, Ying ZC, Ho W. Surf Sci Lett 1991;255:L550.